PROCEEDINGS OF SPIE

SPIEDigitalLibrary.org/conference-proceedings-of-spie

Advantages of concave quantum barriers in AlGaN deep ultraviolet light-emitting diodes

Barsha Jain, Mano Bala Sankar Muthu, Ravi Teja Velpula, Ngoc Thi Ai Nguyen, Hieu Pham Trung Nguyen

Barsha Jain, Mano Bala Sankar Muthu, Ravi Teja Velpula, Ngoc Thi Ai Nguyen, Hieu Pham Trung Nguyen, "Advantages of concave quantum barriers in AlGaN deep ultraviolet light-emitting diodes," Proc. SPIE 12421, Gallium Nitride Materials and Devices XVIII, 124210K (15 March 2023); doi: 10.1117/12.2650411



Event: SPIE OPTO, 2023, San Francisco, California, United States

Advantages of Concave Quantum Barriers in AlGaN Deep Ultraviolet Light-Emitting Diodes

Barsha Jain, Mano Bala Sankar Muthu, Ravi Teja Velpula, Ngoc Thi Ai Nguyen, and Hieu Pham Trung Nguyen*

Department of Electrical and Computer Engineering, New Jersey Institute of Technology, Newark, New Jersey 07102

*Email: hieu.p.nguyen@njit.edu; Phone: 1 973 596 3523

ABSTRACT

Although AlGaN-based deep ultraviolet (UV) light-emitting diodes (LEDs) have been studied extensively, their quantum efficiency and optical output power still remain extremely low compared to the InGaN-based visible color LEDs. Electron leakage has been identified as one of the most possible reasons for the low internal quantum efficiency (IQE) in AlGaN based UV LEDs. The integration of a *p*-doped AlGaN electron blocking layer (EBL) or/and increasing the conduction band barrier heights with prompt utilization of higher Al composition quantum barriers (QBs) in the LED could mitigate the electron leakage problem to an extent, but not completely. In this context, we introduce a promising approach to alleviate the electron overflow without using EBL by utilizing graded concave QBs instead of conventional QBs in AlGaN UV LEDs. Overall, the carrier transportation, confinement capability and radiative recombination are significantly improved. As a result, the IQE, and output power of the proposed concave QB LED were enhanced by ~25.4% and ~25.6% compared to the conventional LED for emission at ~254 nm, under 60 mA injection current.

Keywords: AlGaN, light-emitting diodes, electron-blocking layer, concave, electron leakage

1. INTRODUCTION

AlGaN deep-ultraviolet (UV) light-emitting diodes (LEDs) have undergone extensive research due to their wide range of practical applications [1]. However, current LEDs still exhibit low external quantum efficiency (EQE), which is a function of internal quantum efficiency (IQE), light extraction efficiency (LEE), and carrier injection efficiency (CIE). Large defects and dislocation densities caused by mismatched lattices in the epilayers, the strong polarization-induced quantum-confined Stark effect (QCSE), electron overflow, and poor hole injection efficiency are some of the main reasons causing these problems [2]. To mitigate the electron overflow, an Al-rich p-doped electron-blocking layer (EBL) has been commonly used in between the active region and the p-region [3]. However, at the hetero-interface of the last quantum barrier (QB) and the EBL, a positive polarization sheet charge is generated due to the high Al composition of the EBL layer [4-6]. The hole depletion area is formed at the same interface as a result of the formation of positive sheet polarization charges, leading to the severely limited hole injection efficiency [7, 8]. Additionally, efficient p-doping in Al-rich EBL is challenging due to the high Mg activation energy [9].

Several approaches have been suggested for the reduced electron leakage by using different EBL structures [10-12]. However, the complications associated with these types of EBL structures strongly affect the subsequent epitaxial growth processes. In this paper, we present a promising approach for reducing electron overflow in AlGaN UV LEDs by using EBL-free structure with graded concave QBs instead of conventional QBs. The proposed graded QBs raise the conduction band barrier heights (CBBH), while the concave structure slows hot electrons by lowering the electron mean free path (MFP) before entering the quantum wells (QWs). Overall, the output power, IQE, and radiative recombination of the proposed LED are significantly increased compared to the reference structure.

2. DEVICE STRUCTURE AND PARAMETERS

The reference LED structure, denoted as LED 1, is adopted from Yan et al. [13]. Illustrated in Fig. 1(a), LED 1 contains a 3 μ m n-Al_{0.7}Ga_{0.3}N layer (5×10¹⁸ cm⁻³), five undoped 3 nm Al_{0.6}Ga_{0.4}N QWs sandwiched between six undoped 12 nm Al_{0.7}Ga_{0.3}N QBs as active region, a 20 nm p-Al_{0.8}Ga_{0.15}N (2×10¹⁹ cm⁻³) EBL, a 50 nm p-Al_{0.7}Ga_{0.3}N (2×10¹⁹ cm⁻³) cladding

Gallium Nitride Materials and Devices XVIII, edited by Hiroshi Fujioka, Hadis Morkoç, Ulrich T. Schwarz, Proc. of SPIE Vol. 12421, 124210K © 2023 SPIE · 0277-786X · doi: 10.1117/12.2650411

layer, and a 120 nm p-GaN (1×10²⁰ cm⁻³) contact layer. Figure 1(b) presents the Al composition profile information for the conduction band of LED 1. The proposed LED with concave QBs is denoted as LED 2. There are two specific changes in LED 2, compared to the reference structure, LED 1. The conventional EBL layer is not presented in LED 2 and the regular QBs are replaced with concave QBs. The proposed concave QBs are composed of 4 nm Al_xGa_{1-x}N/4 nm Al_{x-0.03}Ga_{1-(x-0.03)}N/4 nm Al_xGa_{1-x}N layers along the growth direction. The values of x for five QBs are 0.65, 0.68, 0.71, 0.74, and 0.77, respectively. This can be seen from Fig. 1(c). The mesa area of both LEDs is considered as 400 × 400 μ m².

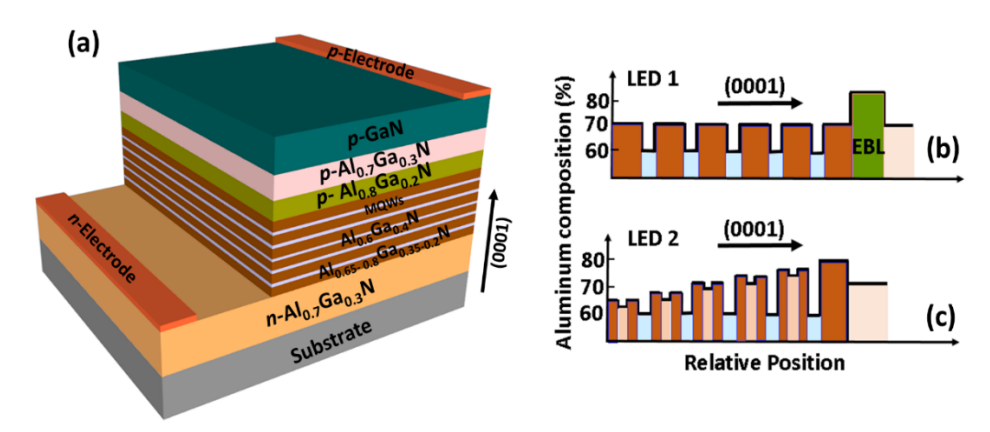


Figure 1. (a) Schematic representation of LED 1, Al composition (%) profile related to the conduction band of (b) conventional structure, i.e., LED 1, and (c) proposed LED structure, i.e., LED 2.

The Mg activation energy for the p-Al_xGa_(1-x)N alloy is determined by using a linear approximation. It is considered as 170 meV for p-GaN and 510 meV for p-AlN, respectively [14]. The net polarization caused by piezoelectric and spontaneous polarization is calculated and set as 50% of the theoretical values [15]. The Shockley-Read-Hall (SRH) recombination coefficient, radiative recombination coefficient, light extraction efficiency, and auger recombination coefficient are set as 6.67×10^7 /s, 2.13×10^{-11} cm³/s, 15%, and 2.88×10^{-30} cm⁶/s, respectively [16]. The band offset ratio for the III-nitride material hetero-junctions is taken as 0.67/0.33 [12]. The energy-band diagrams of two LED structures are calculated using the 6×6 k.p model [17], and other band parameters utilized in our model can be found elsewhere [18]. Moreover, by closely comparing our simulation results for LED 1 with experimental data, we strictly calibrated our simulation parameters and model [13].

3. RESULTS AND DISCUSSION

The calculated energy-band (E-B) diagrams of LED 1 and LED 2 are shown in Fig. 2. The E-B diagrams are estimated at 60 mA injection current. As shown in Table 1, the corresponding CBBH values (ϕ_{en}) at the corresponding barrier (n) of the conduction bands for the proposed structure, LED 2, are gradually increasing as compared to that of the conventional structure, LED 1. This would improve the electron blocking capability in the active region and reduce the electron leakage into the *p*-region [4].

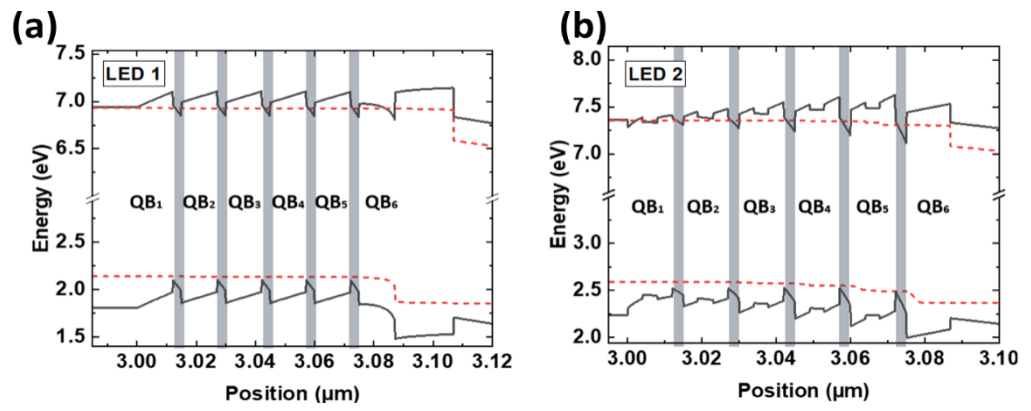


Figure 2. Energy band diagram of (a) LED 1 and (b) LED 2 at 60 mA injection current.

Moreover, the presence of concave QBs in LED 2 would slow down the hot electrons by lowering the electron MFP before entering into quantum wells in the active region which would play an additional role in reducing the electron leakage [19]. Next, the effective valence band barrier height (VBBH) values (ϕ_{hn}) at the corresponding barrier (n) of the valence band are estimated and presented in Table 2. It is found that the ϕ_{hn} values are gradually increasing in the proposed LED structure, LED 2, compared to LED 1 due to increase in Al composition in the QBs. It is anticipated that this would support in improving the hole confinement in the active region.

Table 1. Effective CBBHs of QBs (\$\phi_{en}\$) for LED 1 and LED 2.

СВВН	LED 1	LED 2
фе1	174.7 meV	56.74 meV
фе2	179.3 meV	123.3 meV
фез	178.8 meV	194.3 meV
фе4	173.3 meV	259.6 meV
фе5	173.2 meV	323.2 meV
фе6	46.6 meV	232.9 meV

Table 2. Effective VBBHs of QBs (φhn) for LED 1 and LED 2.

VBBH	LED 1	LED 2
ф _{h2}	281.4 meV	259.8 meV
фь3	280.2 meV	322.6 meV
ф _{h4}	279.6 meV	374.5 meV
фь5	277.1 meV	428.3 meV

The electron concentrations in the active region of LED 1 and LED 2 are depicted in Fig. 3(a). As expected, the reduced electron mean free path improves electron concentration in the active region of LED 2. The integrated electron densities in LED1 and LED 2 are 5.8×10^{12} cm⁻² and 9.2×10^{12} cm⁻². As a result, electron overflow from LED 2 active region is reduced when compared to LED 1. Therefore, lower electron leakage was discovered in the *p*-region of LED 2, as illustrated in Fig. 3(b). The reduced electron leakage also prevents undesirable non-radiative recombination of leaked electrons with incoming holes in the *p*-region. It also facilitates the hole injection into the multi QWs. Furthermore, effective VBBHs in LED 2 supports better hole transport among the QWs. Altogether, the overall hole concentration in the active region of LED 2 is increased and shown in Fig. 3(c). The integrated electron densities in LED1 and LED 2 are 4.4×10^{12} cm⁻² and 4.9×10^{12} cm⁻². Subsequently, radiative recombination is also significantly improved due to the higher carrier concentration in the multi QWs of LED 2 compared to LED 1. This is provided in Fig. 3(d).

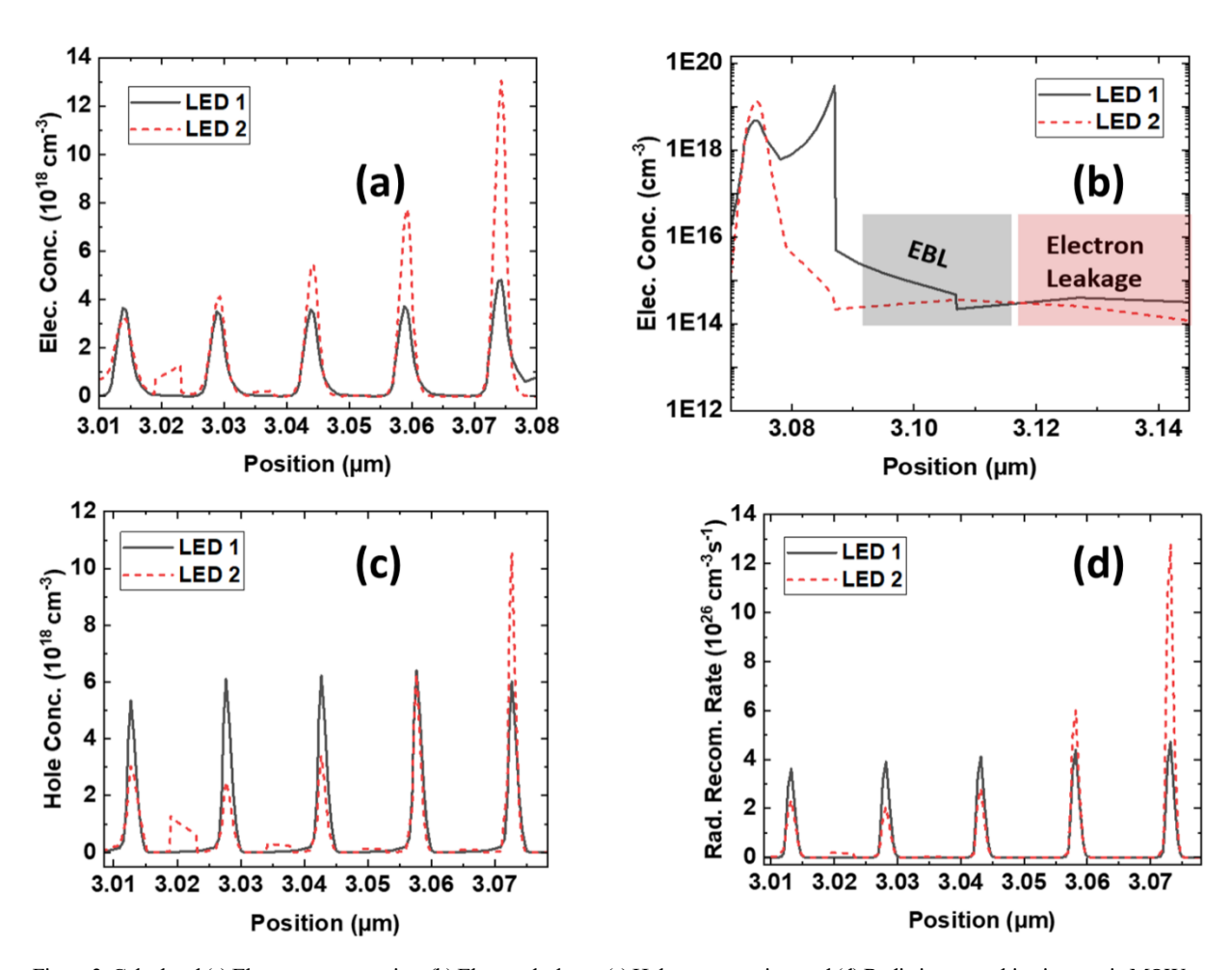


Figure 3. Calculated (a) Electron concentration, (b) Electron leakage, (c) Hole concentration, and (d) Radiative recombination rate in MQWs of LED 1 and LED 2.

The IQE of both LEDs is calculated further, as shown in Fig. 4. (a). LED 2 has a maximum IQE of 31%, whereas LED 1 has a maximum IQE of 20% due to the improved radiative recombination and reduced electron overflow. Furthermore, at 60 mA injection current, LED 2 has a 25.4% higher IQE than LED 1. The electroluminescence (EL) spectra of both LEDs are depicted in Fig. 4(b). Again, the EL intensity of LED 2 is higher than that of LED 1 at the emission wavelength of 254 nm due to the improved radiative recombination.

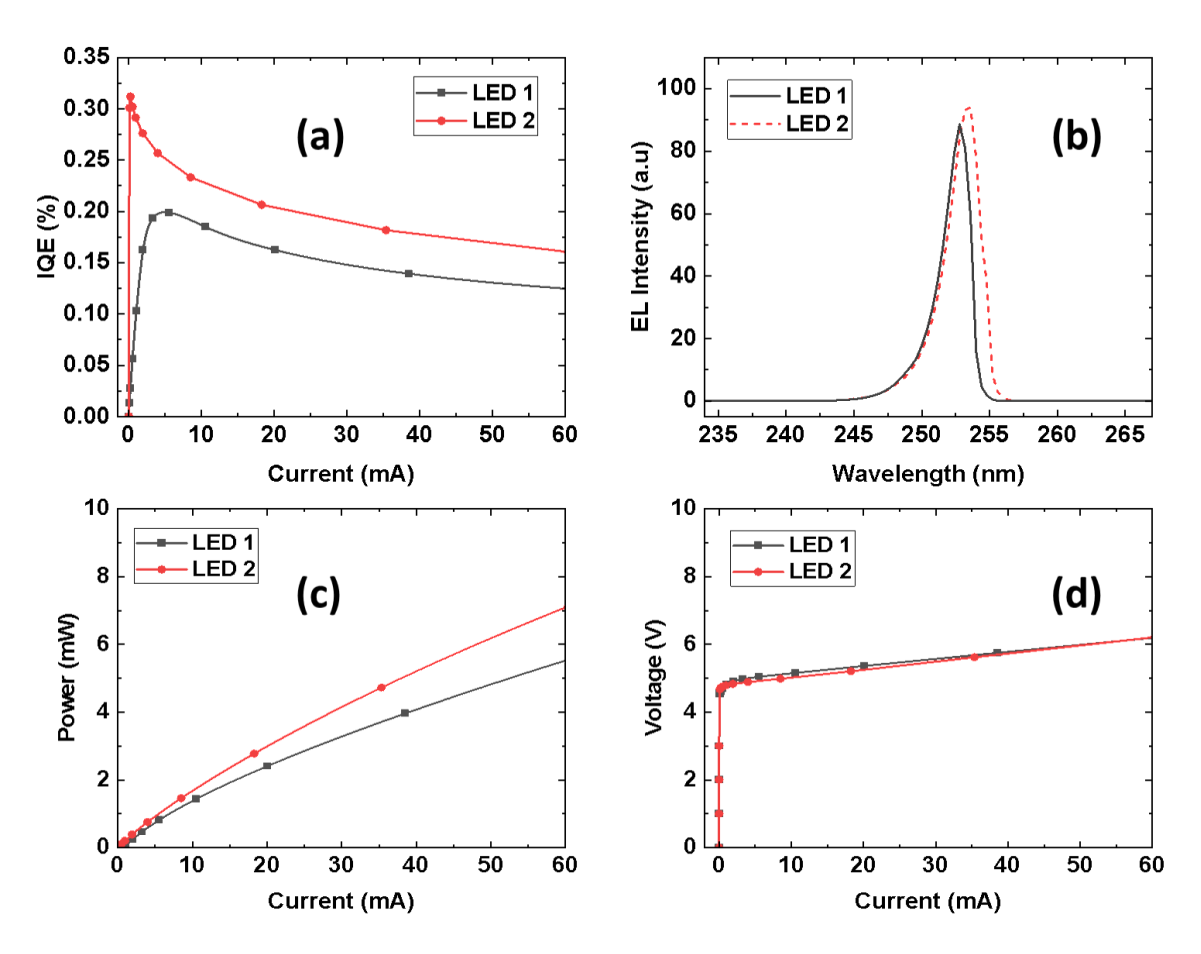


Figure 4. Calculated (a) IQE-current characteristics, (b) EL intensity, (c) Power-current characteristics, and (d) Voltage-current characteristics of LED 1 and LED 2.

Figures 4(c) and 4(d) show the power vs. current (L-I) and voltage vs. current (I-V) characteristics of LED 1 and LED 2. LED 2 has a nearly identical turn-on voltage to LED 1, with a slightly higher operating bias voltage at 60 mA injection current. However, the output power of LED 2 has increased dramatically. LED 2 has a recorded output power of 10.3 mW at 60 mA current injection, which is 25.6% higher than LED 1 at the same injection current level.

4. CONCLUSION

We have reported the advantages of utilization of graded concave QBs instead of conventional QBs in AlGaN deep UV LEDs. The proposed LED structure could be able to notably slow down the hot electrons thereby reducing the electron thermal velocity and mean free path which greatly improved the carrier confinement in the QWs and significantly reduced the electron overflow from the active region. As a result, the proposed LED with concave QBs exhibited improved IQE, and output power by \sim 25.4% and \sim 25.6% respectively, compared to the conventional LED at 60 mA injection current.

5. ACKNOWLEDGEMENTS

This study was funded by the US National Science Foundation, under grant number ECCS-1944312, and the New Jersey Health Foundation, under grant number PC 24-22.

REFERENCES

- [1] M. Kneissl, T.-Y. Seong, J. Han, and H. Amano, "The emergence and prospects of deep-ultraviolet light-emitting diode technologies," *Nature Photonics*, vol. 13, no. 4, pp. 233-244, 2019.
- [2] J. Cho, E. F. Schubert, and J. K. Kim, "Efficiency droop in light-emitting diodes: Challenges and countermeasures," *Laser & Photonics Reviews*, vol. 7, no. 3, pp. 408-421, 2013.
- [3] H. Hirayama *et al.*, "222–282 nm AlGaN and InAlGaN-based deep-UV LEDs fabricated on high-quality AlN on sapphire," *Physica Status Solidi (a)*, vol. 206, no. 6, pp. 1176-1182, 2009.
- [4] R. T. Velpula, B. Jain, S. Velpula, H.-D. Nguyen, and H. P. T. Nguyen, "High-performance electron-blocking-layer-free deep ultraviolet light-emitting diodes implementing a strip-in-a-barrier structure," *Optics Letters*, vol. 45, no. 18, pp. 5125-5128, 2020.
- [5] R. T. Velpula, B. Jain, T. R. Lenka, R. Wang, and H. P. T. Nguyen, "Polarization-Engineered p-Type Electron-Blocking-Layer-Free III-Nitride Deep-Ultraviolet Light-Emitting Diodes for Enhanced Carrier Transport," *Journal of Electronic Materials*, vol. 51, no. 2, pp. 838-846, 2022.
- [6] H. Q. T. Bui *et al.*, "Enhancing Efficiency of AlGaN Ultraviolet-B Light-Emitting Diodes with Graded p-AlGaN Hole Injection Layer," *Physica Status Solidi (a)*, vol. 218, no. 15, p. 2100003, 2021.
- [7] R. T. Velpula *et al.*, "Improving carrier transport in AlGaN deep-ultraviolet light-emitting diodes using a strip-in-a-barrier structure," *Applied Optics*, vol. 59, no. 17, pp. 5276-5281, 2020.
- [8] B. Jain, R. T. Velpula, M. Patel, S. M. Sadaf, and H. P. T. Nguyen, "Improved Performance of Electron Blocking Layer Free AlGaN Deep Ultraviolet Light-Emitting Diodes Using Graded Staircase Barriers," *Micromachines*, vol. 12, no. 3, p. 334, 2021.
- [9] M. Nakarmi, N. Nepal, J. Lin, and H. Jiang, "Photoluminescence studies of impurity transitions in Mg-doped AlGaN alloys," *Applied Physics Letters*, vol. 94, no. 9, p. 091903, 2009.
- [10] Y. Li et al., "Advantages of AlGaN-based 310-nm UV light-emitting diodes with Al content graded AlGaN electron blocking layers," *IEEE Photonics Journal*, vol. 5, no. 4, pp. 8200309-8200309, 2013.
- [11] Z.-H. Zhang *et al.*, "Nearly efficiency-droop-free AlGaN-based ultraviolet light-emitting diodes with a specifically designed superlattice p-type electron blocking layer for high mg doping efficiency," *Nanoscale Research Letters*, vol. 13, no. 1, pp. 1-7, 2018.
- [12] B. Jain, R. T. Velpula, S. Velpula, H.-D. Nguyen, and H. P. T. Nguyen, "Enhanced hole transport in AlGaN deep ultraviolet light-emitting diodes using a double-sided step graded superlattice electron blocking layer," *JOSA B*, vol. 37, no. 9, pp. 2564-2569, 2020.
- [13] J. Yan *et al.*, "AlGaN-based deep-ultraviolet light-emitting diodes grown on high-quality AlN template using MOVPE," *Journal of Crystal Growth*, vol. 414, pp. 254-257, 2015.
- [14] K. Nam, M. Nakarmi, J. Li, J. Lin, and H. Jiang, "Mg acceptor level in AlN probed by deep ultraviolet photoluminescence," *Applied Physics Letters*, vol. 83, no. 5, pp. 878-880, 2003.
- [15] V. Fiorentini, F. Bernardini, and O. Ambacher, "Evidence for nonlinear macroscopic polarization in III–V nitride alloy heterostructures," *Applied Physics Letters*, vol. 80, no. 7, pp. 1204-1206, 2002.
- [16] J. Yun, J.-I. Shim, and H. Hirayama, "Analysis of efficiency droop in 280-nm AlGaN multiple-quantum-well light-emitting diodes based on carrier rate equation," *Applied Physics Express*, vol. 8, no. 2, p. 022104, 2015.
- [17] S. Chuang and C. Chang, "k· p method for strained wurtzite semiconductors," *Physical Review B*, vol. 54, no. 4, p. 2491, 1996.
- [18] I. Vurgaftman and J. n. Meyer, "Band parameters for nitrogen-containing semiconductors," *Journal of Applied Physics*, vol. 94, no. 6, pp. 3675-3696, 2003.
- [19] B. Jain, R. T. Velpula, M. Patel, and H. P. T. Nguyen, "Controlled carrier mean free path for the enhanced efficiency of III-nitride deep-ultraviolet light-emitting diodes," *Applied Optics*, vol. 60, no. 11, pp. 3088-3093, 2021.